International Journal of Engineering &Technology, 13 (1) (2024) 1-12

International Journal of Engineering & Technology

Website: www.sciencepubco.com/index.php/IJET

Research paper

Modeling of a photovoltaic drip irrigation system for an offseason crop: case of onion cultivation in PITOA (North Cameroon)

Boussaibo Andre[1]*, Sawalda Alphonse[2], Ndjiya Ngasop Stephane[2], Deli Goron[3], Pene Armel Duvalier[1], Kitmo[3]

[1]Department of Electrical Engineering, University Institute of Technology University of Ngaoundere, Cameroon
[2]Department of Electrical Engineering, Energy and Automation, National School of Agro-Industrial Sciences, University of Ngaoundere, Ngaoundere, Cameroon
[3]Department of Renewable Energy, National Advanced School of Engineering University of Maroua,
**Corresponding author E-mail:boussaibo@yahoo.fr*

Abstract

In this article, attention is paid to the use of photovoltaic electricity for the popularization of off-season agriculture in arid Sahelian areas. Here we propose an efficient solar drip irrigation model for rational use of water for off-season crops. The model of the proposed sys-tem is developed in the MATALAB/Simulink environment. The results of simulations based on field data specific to the cultivation of off-season onions in the locality of PITOA (North Cameroon) are obtained for a cultivable area of 1 hectare, according that the area to be irrigated is 7200 m². The algorithm developed for determining the soil capacity made it possible to evaluate the useful reserve at 1.70 mm/cm. Under the set test conditions (temperature 25°C, irradiance 1000 W/m²), the water flow provided by a dripper is estimated at 20 l/h. To meet the water needs of crops, the power of the photovoltaic generator is 1600 W peak.

Keywords: *Photovoltaic Pumping; Drip Irrigation; Onion Cultivation; Sahelian Zones.*

1. Introduction

Climate change poses a growing threat to food security on the African continent, mainly because of its effect on the length of the season in which farmers can grow crops. The World Food Program's Global Report on Food Crises indicates that the number of people in Africa experiencing acute food insecurity and in need of humanitarian assistance in 2020 increased by almost 40% compared to 2019 to reach almost 100 million (World Bank, 2020). This situation is partly caused by the reduction in crop yields in several African countries, due to insufficient rains. One of the possible solutions is the promotion and popularization of adapted improved seeds that do not require a long period of rain in order to reach maturity. But unfortunately, because of the prevailing precariousness, people have difficulty accessing it. Another possible solution to encourage and popularize is the promotion of off-season crops (Diwediga and al., 2012). By adopting out-of-season crops, farmers generally use various techniques for irrigating crops: manual watering, pumping with a thermal engine or pumping with human or animal power (ARID, 2007). These irrigation techniques coupled with water scarcity during dry seasons are tedious, expensive and consume water, which is already insufficient. The practice of efficient irrigation, in particular drip irrigation coupled with the use of photovoltaic energy, seems more suitable and appropriate for off-season crops given the importance of the solar resource in this area, i.e. 5.8 KWh/J/m² (Ayangma and al., 2008). In this research work, the objective is to propose a drip irrigation system, having photovoltaic electricity as an energy source and applied to the cultivation of onions. The system in question is made up of a photovoltaic field, a DC-DC voltage boost converter and its control algorithm, a direct current motor, a centrifugal pump and an irrigation network.

2. Materials and methods

2.1. Study site

The study site that served as a benchmark for this research work is located in PITOA. Geographically, PITOA is a locality in northern Cameroon with coordinates 9°23′NORTH and 13°32′EAST. It is renowned for being a large basin of off-season crops and more particularly the cultivation of onions (M'Biandoun and Essang, 2008). The data base necessary for the analyzes and simulations as part of this work was drawn from this locality. These include the results of surveys of local farmers, samples of arable land, plot distribution models and crop durations.

2.2. Synoptic of the irrigation system

Copyright ©Boussaibo Andre et al. This is an open access article distributed under the Creative Commons Attribution License, which permits unrestricted use, distribution, and reproduction in any medium, provided the original work is properly cited.

The diagram in Figure. 1 presents the synoptic of the irrigation system which constitutes the basis of this research work. It is made up of two large electrical and hydraulic blocks. The electrical block is composed of the PV generator, the PWM control, the BOOST converter and the motor. The hydraulic block is made up of the pump, the irrigation network and the surface to be irrigated materialized in water requirement.

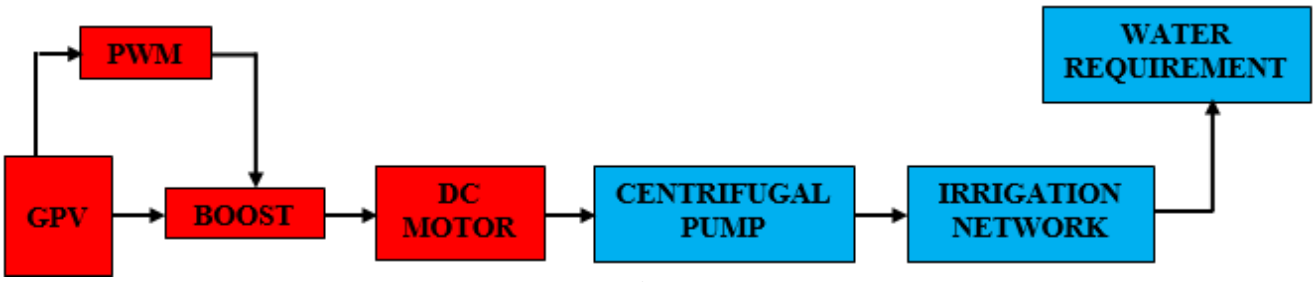


Fig. 1: Synoptic of the Irrigation System.

2.3. Calculations of the factors that influence the irrigation system

2.3.1. Determination of soil capacity

Determining the capacity of the soil consists of evaluating the reserve of easily usable water by the soil to be irrigated. In fact, the useful reserve (RU) corresponds to the retention capacity of the soil, that is to say the volume of water that the soil can absorb and expressed in mm of water per centimetre of fine soil, i.e., mm/cm. The useful reserve depends on the texture of the soil (which characterizes the nature, size and distribution of the solid particles which constitute it) and on the structure of the soil (which characterizes the way in which the solid elementary particles or aggregates are associated). Regarding the structure of the soil, the determination method is as Figure. 2 follows (Maud Du Jardin, 2022):

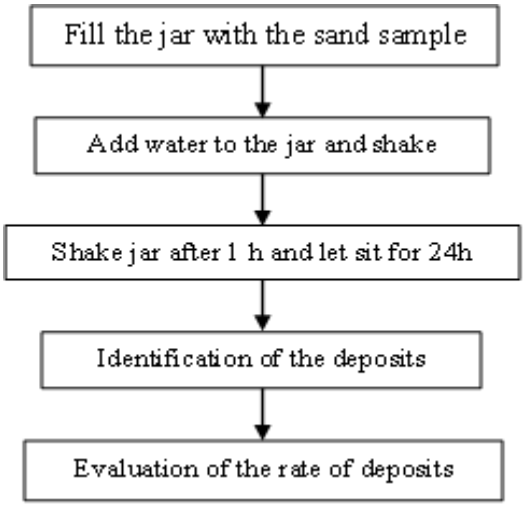


Fig. 2: Flowchart for Determining Soil Structure.

As for the texture of the soil, we rely on the diagram in Figure. 3 below which represents the texture triangle (Duchaufour and al., 2018).



Fig. 3: Texture Triangle.

The following equation gives the expression for the final capacity of the soil:

$$RFU_{Horizon} = RF.PEC \quad (1)$$
$$RFU_{Horizon} = RF.PEC$$

Where:$RFU_{Horizon}$ final soil capacity
RFU: the easily usable reserve
PEC: the rooting depth of the soil

2.3.2. Water requirement

At each phase of a plant's growth, water requirements vary, for each crop and according to the different periods of vegetative development (Youssouf and al., 1999), because the water consumption of crops depends on different climatic elements: temperature, air humidity, wind and sunshine. A supply of water in quantities greater or less than the plants' needs has a negative impact on production yield. Calculating the right dose of water to provide to the crop is essential for sizing a drip irrigation system. The following equation presents the expression of the water requirement for a given plant:

$$BN = (ETM - P_e)E_g \quad (2)$$

With: BN: water requirement (mm/month)
ETM: Maximum evapotranspiration (mm/month)
P_e: Effective rain (mm/month)
E_g: Overall efficiency (%)

Maximum evapotranspiration is calculated from potential evapotranspiration (ETP) and the crop coefficient (K_c) following the expression of the equation follow (Allen et al., 2006):

$$ETM = ETP.K_c \quad (3)$$

Potential evapotranspiration which is defined as the quantity of water evaporated by the soil and by the plant is given by the Penman-Monteith method so the expression is that of the following equation:

$$\text{ETP} = \frac{0{,}408\Delta(R_n - G)d + \gamma\frac{900}{T_{aver}+273}\mathcal{V}(e_\omega - e)}{\Delta + \gamma(1+0{,}34\mathcal{V})} \quad (4)$$

Where:

$$\Delta = \frac{4098\left[0.6108exp\left(\frac{17.27T_{aver}}{T_{aver}+237.3}\right)\right]}{(T_{aver}+237.3)^2} \quad (5)$$

$$e_w = \frac{e_w(T_{max}) + e_w(T_{min})}{2} \quad (6)$$

$$e = \frac{e_w(T_{min})\frac{H_{rmax}}{100} + e_w(T_{max})\frac{H_{rmin}}{100}}{2} \quad (7)$$

$$\gamma = 0.665\,X\,10 - 3P \quad (8)$$

The following equation presents the expression for the crop coefficient proposed by Allen:

$$K_c = K'_c + [0.04(\mathcal{V} - 2) - 0.004(H_{raver} - 45)]\left(\frac{HMC}{3}\right)^{0.3} \quad (9)$$

With: k'_c: coefficient of bibliographic culture;
k_c : culture coefficient adapted to the environment;
$\mathcal{V}$: daily average wind value at 2m height (m/s);
H_{raver}: average value of relative humidity (%);
HMC: average height of the crop (m).

2.3.3. Irrigation network

The diagram in Figure. 4 below illustrates the irrigation network applicable to onion cultivation as practiced by farmers.

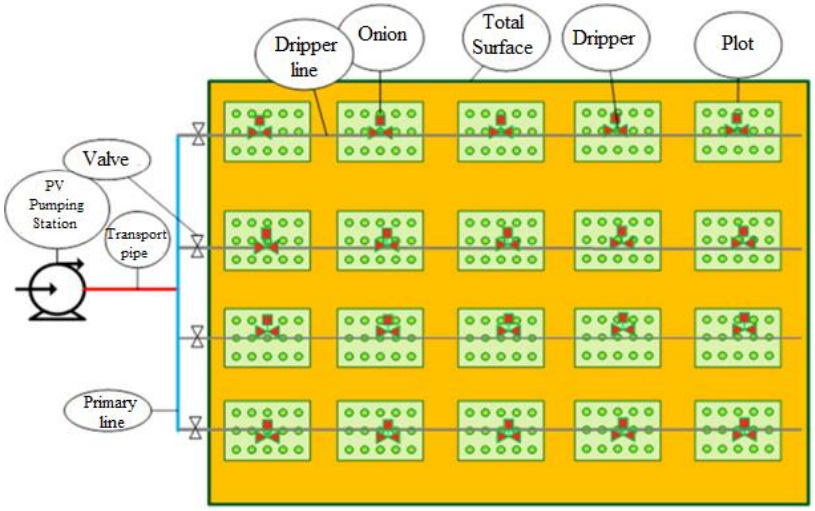


Fig. 4: Irrigation Network.

This network is made up of the following main elements:

- A transport pipe connected to the photovoltaic pumping system;
- A primary line pipe connected perpendicular to the transport line which supplies the dose to the dripper lines;
- Pipes called dripper lines which carry the drippers delivering the dose to the onion roots;
- Hydraulic accessories ensuring various functions on the network.

2.3.4. Pipe sizing

Given the strong sunlight in the study area, the pipes must be made of material with anti-UV protection and which is suitable for drip irrigation. In general, pipe sizing is done on the basis of the following elements:

- Flow speed: it must be taken between 0.6 and 1.7 m/s to avoid overpressure in the pipes;
- Diameter of the pipes: it must allow the peak flow to be conveyed while not creating enormous pressure losses; it can be obtained by the following relation:

$$D = \sqrt{\frac{4Q}{\pi V}} \tag{10}$$

Singular pressure losses are taken equal to 10% of linear pressure losses; knowing that the linear pressure losses are given by the following relationship:

$$\Delta H_L = \Delta H_{simple} \,.\, F.L \tag{11}$$

Where:

$$\Delta H_{simple} = \frac{a}{1000} . \frac{Q^N}{D^M} \tag{12}$$

The singular load losses are then such that:

$$\Delta H_S = \Delta H_L . 10\% \tag{13}$$

The total pressure losses in the pipes result from the sum of the linear pressure losses and the singular losses according to the following formula:

$$\Delta H = \Delta H_L + \Delta H_S \tag{14}$$

The pressure difference across the system must be such that a high degree of watering uniformity is achieved. To ensure this, the Christiansen criterion proposes a relationship valid for all pressure systems:

$$\Delta h = 20\%. P_{nom} \tag{15}$$

2.4. Centrifugal pump modeling

The diagram in Figure. 5 below illustrates the electrical modelling of a direct current motor according to Bouadi and al., (2015). It can be compared to a system whose input is the armature control voltage u(t) and the output the rotation speed of the motor shaft $\omega_m(t)$. The armature is modeled by a resistance in series with an inductance and a counter electromotive force:

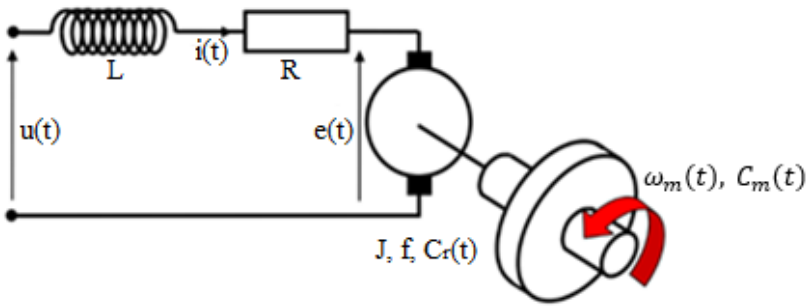


Fig. 5: Model of an Electric Current Motor.

The mathematical model of this engine is given by the following system of equations:

$$\begin{cases} u(t) = e(t) + Ri(t) + L\frac{di(t)}{dt} \\ e(t) = K_e.\omega_m(t) \\ j.\frac{d\omega_m(t)}{dt} = c_m(t) - c_r(t) - f.\omega_m(t) \\ c_m(t) = K_t.i(t) \end{cases} \quad (16)$$

This mathematical model is a system of coupled differential equations, difficult to solve in this form. By applying the Laplace transform, we obtain a linear system of algebraic equations as follows:

$$\begin{cases} U = E + RI + sL\big(I + i(0)\big) \\ E = K_e\Omega \\ sJ\Omega - J\omega_m(0) = F(C_m) - F(C_r) - f\Omega \\ F(C_m) = K_m I \end{cases} \quad (17)$$

Figure. 6 is the Simulink models of the DC motor based on equations 16 and 17.

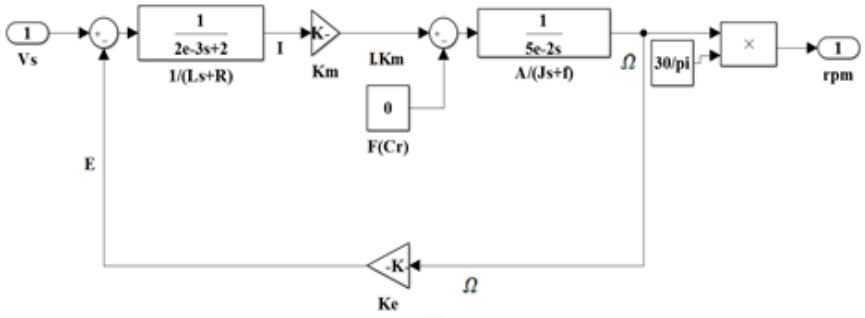


Fig. 6: Simulink Models of the DC.

The centrifugal pump model that we will apply is that of the law of similarity (Elmahni and al., 2016). Knowing the performances of a centrifugal pump (Flow rate (Q), Total head (H) and Motor power (P)) for the rotation frequency (N), the laws of similarity make it possible to determine the new performances (Q', H' and P') for a frequency (N') as follows:

$$Q' = \frac{N'}{N}Q \;; \qquad H' = \left(\frac{N'}{N}\right)Q^2 \;; \qquad P' = \left(\frac{N'}{N}\right)P^3 \quad (18)$$

Figure. 7 is the Simulink models of the centrifugal pump based on equation 18.

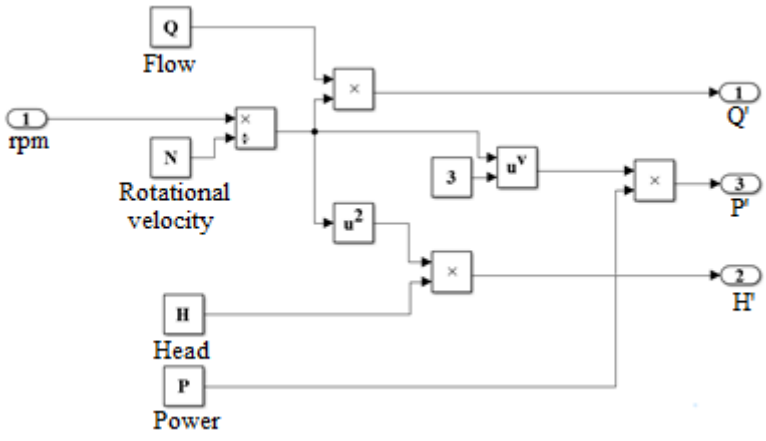


Fig. 7: Simulink Model of the Centrifugal Pump.

2.5. PV field modelling

In this study, we will consider the model of the single-diode PV cell as illustrated by the diagram in Figure 8.

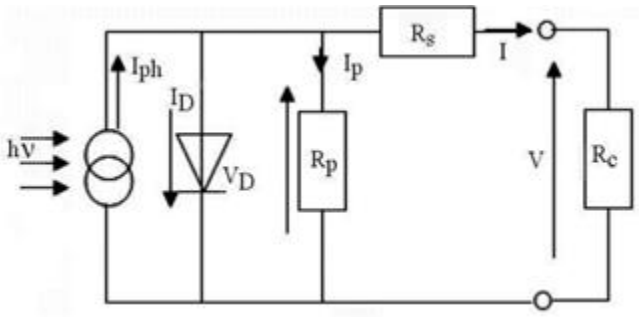


Fig. 8: Equivalent Model of the Solar Cell with a Diode.

Applying Kirchhoff's laws to this circuit, the current I delivered by the cell is the algebraic sum of three currents:

$$I = I_{ph} - I_D - I_p \tag{19}$$

The voltage across the diode is:

$$V_D = R_p . I_p = V + R_s . I \tag{20}$$

Where Ip represents the current passing through the parallel resistance, R_p

$$I_p = \frac{V+R_s.I}{R_p} \tag{21}$$

The current of the diode I_D is therefore written in the form:

$$I_D = I_0 \left[exp\left(\frac{V+R_S*I}{A.K.T}\right) - 1 \right] \tag{22}$$

$$I_0 = I_{rs} \left[\frac{T}{T_{ref}}\right]^3 exp\left(\frac{qE_{g0}(\frac{1}{T_{ref}} - \frac{1}{T})}{AK}\right) \tag{23}$$

$$I_{rs} = I_{scref} \cdot \frac{1}{e^{\left(\frac{qV_{oc}}{AKT}\right)} - 1} \tag{24}$$

The photocurrent I_{ph} has the expression:

$$I_{ph} = \frac{G[I_{Scref} + K_i(T_c - T_{ref})]}{G_{ref}} \tag{25}$$

By replacing the currents in equation 19 with their expressions 21, 22 and 25, we obtain the equation of the I(V) characteristic of the photovoltaic cell:

$$I = \frac{G[I_{Scref} + K_i(T - T_{ref})]}{Gref} - \left(I_{scref} \cdot \frac{1}{e^{\left(\frac{qV_{oc}}{AKT}\right)} - 1}\right)\left(\left[\frac{T}{Tref}\right]^3 exp\left(\frac{qE_{g0}\left(\frac{1}{T_{ref}} - \frac{1}{T}\right)}{AK}\right)\right)\left[exp\left(\frac{V+R_S I}{AV_T}\right) - 1\right] - \frac{V+R_S I}{R_p} \tag{26}$$

For a photovoltaic field made up of N_p modules in parallel and N_s modules in series, the expression of the characteristic I(V) of the PV module is deduced from that of the cell.

$$I = N_p I_{ph} - N_p I_0 \left[exp\left(\frac{q(V+R_s I)}{AKT N_s}\right) - 1\right] - \left(\frac{V+IR_s}{R_p}\right) \tag{27}$$

The following diagram in Figure. 9 is the Simulink model of the photovoltaic field based on equations 27.

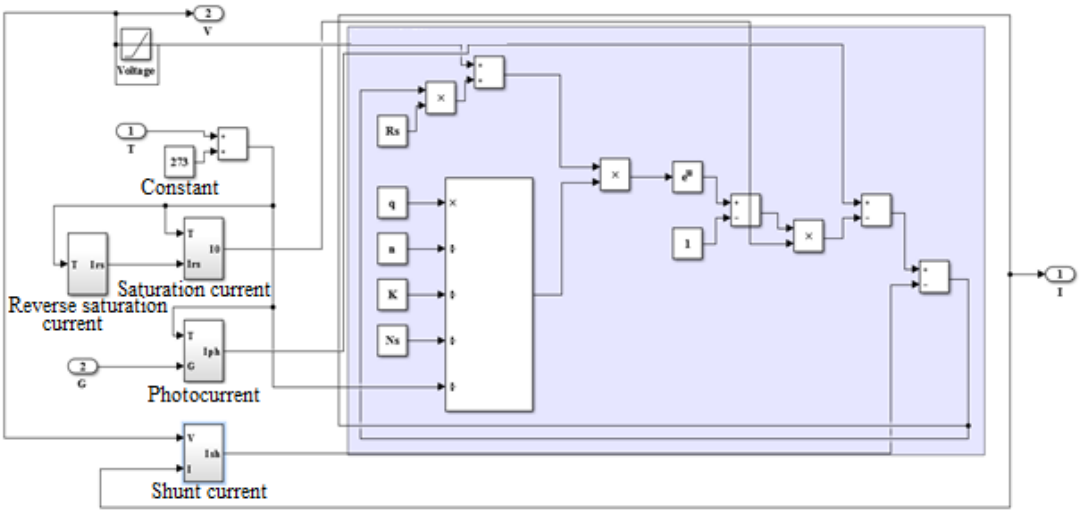


Fig. 9: Simulink Model of the PV Module.

2.6. Modelling the boost converter

The Boost converter must be able to raise the voltage of the photovoltaic field to the nominal operating voltage of the pump. For a voltage across the photovoltaic generator V_e=48 V and the switching frequency f=500 Hz the characteristics of the Boost components are as follows:

- $L = 1{,}87 * 10^{-3} H$
- $C = 2{,}83 * 10^{-3} F$

The schematic in the following Figure. 10 is the Simulink model of the boost converter.

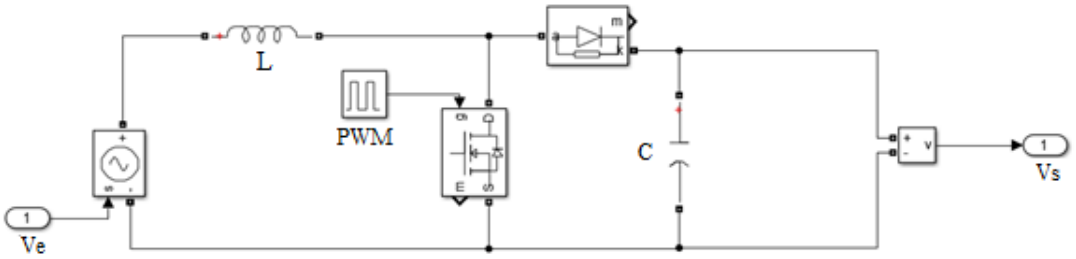


Fig. 10: Simulink Model of the Boost Converter.

The PWM signal is provided by the P&O control algorithm illustrated in the diagram in Figure. 11 below.

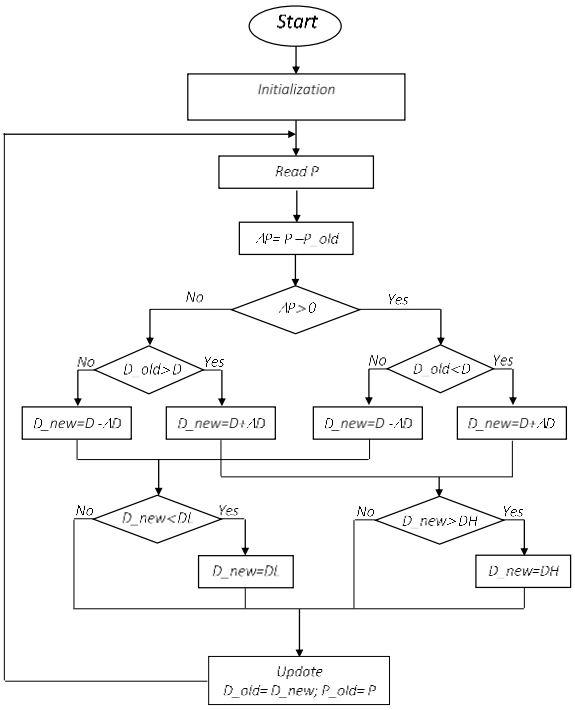


Fig. 11: Control Algorithm.

2.7. Simulink model of the overall system

The Simulink model of the overall system is that of Figure.12 below. It results from the interconnection of the different components of the irrigation system. These are the photovoltaic generator, the Boost converter, the direct current motor, the centrifugal pump, and the irrigation network.

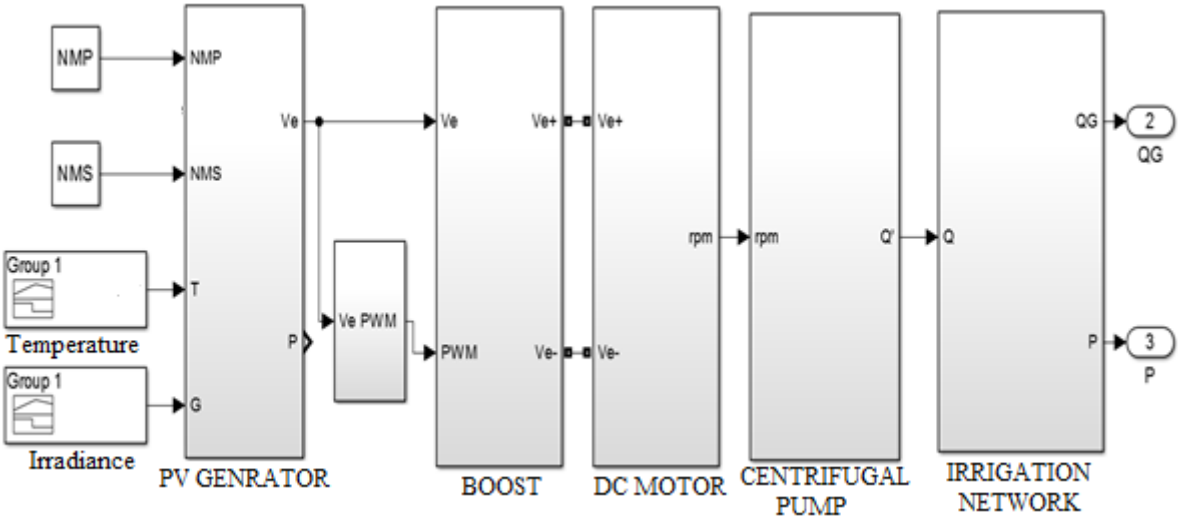


Fig. 12: Simulink Model of the Complete Simplified System.

3. Sizing results

3.1. Irrigation network

3.1.1. Soil capacity

Figure. 13 below show the soil texture of the study area. This texture is that of a Clay-Sandy soil with regard to the proportions of the different components (Sieffermann, 1964). For this purpose, the easily usable reserve is therefore: RFU=1.13 mm/cm. The total volume of water that the study area is capable of retaining is 244.800 L.

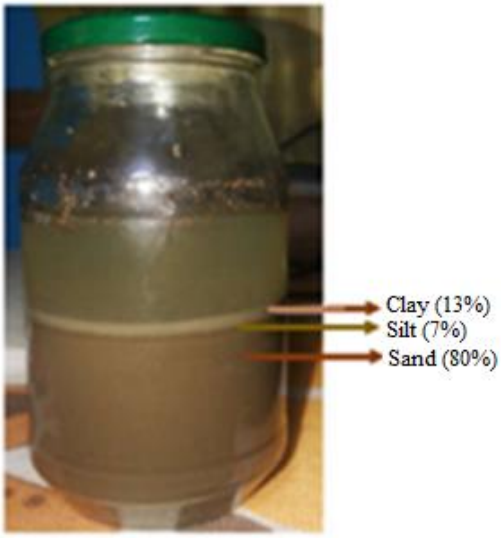


Fig. 13: Proportions of Clay, Silt and Sand in the Soil of the Study Area.

3.1.2. Plot configuration

Table 1 summarizes the field data specific to the surface to be irrigated. These data are inspired by the practical habits of local farmers except for the number of dripper lines which is a component specific to the irrigation technique that we apply.

Table 1: Characteristics of the Plots

Designation	Values
Surface area of a plot (m²)	12
Total surface area to be irrigated (m²)	7200
Spacing between plots (m)	0.5
Spacing between plot and edges (m)	0.25
Number of dripper lines	40

3.1.3. Assessment of water need

Two onion growing seasons exist in the study area. A first season running from October to January and a second season running from November to February. As part of this work, we are interested in the first season. Determining the water requirement (ETM) gives us the results summarized in Table 2 below.

Table 2: Monthly Water Requirement for Onion Cultivation in the Study Area

	October	November	December	January
ETM (mm/month)	131.41±1.31	188.62±2.63	193.61±2.71	216.63±2.55
ETM (mm/day)	4.24±0.01	6.29±0.09	6.25±0.05	6.98±0.15

Analysis of this table allows us to see that the need for water increases over the months of cultivation. This can be justified by the increasing demand for water with plant growth. On the other hand, the first months of cultivation still benefit from the latest rains.

3.1.4. Pipe dimensions

Table 3 below presents the characteristics of the pipes necessary for irrigation of the total surface area to be irrigated, i.e. 7200 m².

Table 3: Pipe Characteristics

Conduit	Dripper line	Primary line	Transmission line
Number	40	1	1
Total flow (L/min)	15	600	600
Total pressure losses (m)	1.97	0.385	0.055
Length (m)	99.5	97.5	5
Standardized diameter (mm)	20	110	110

3.2. Centrifugal pump characteristics

Table 4 summarizes the electrical, hydraulic and mechanical parameters of the centrifugal pump used to supply water to the surface to be irrigated. The values thus obtained are the optimum values of the parameters to allow the centrifugal pump to provide the water flow necessary for the drippers according to the water needs of the plants.

Table 4: Pump Parameters

Designation	Values
Flow(m3/h)	36
Head (m)	14
Maximum current (A)	14
Minimum motor operating voltage (V)	102
Rated motor operating voltage (V)	110
Yield (%)	98
Rated motor power (kW)	1.5
Minimum rotation speed (rpm)	900
Maximum rotation speed (rpm)	3300

3.3. Characteristics of the photovoltaic module

The photovoltaic module used as part of this sizing work is the one whose characteristics are presented in table 5 below. In order to provide the pump with the necessary nominal power, eight modules with these characteristics are coupled in parallel/series so as to obtain an output voltage of 48 V (Boost input voltage) and an output current of at least of 32 A. The total power of the field is thus 1600 W.

Table 5: Photovoltaic Module Parameters

Designation	Values
Maximum power Pm (W)	200
Open circuit voltage V_{OC} (V)	57.6
Short circuit current I_{SC} (A)	4.6
Voltage at P_m, V_{mp} (V)	47.06
Courrent at P_m, I_{mp} (A)	4.25
Numbers of cells in series	96

4. Simulation results

4.1. Influence of clay/silt on soil capacity

Figure. 14 represents the soil capacity (RFUh) as a function of the proportion of clay and silt. Comparing the results of this figure to the texture triangle, we see that the values obtained are consistent for the onion rooting depth of 30 cm. Furthermore, the greater the proportion of clay, the lower the capacity of the soil. Conversely, the greater the proportion of silt, the greater the capacity of the soil. The exploitation of the results of this table shows that the capacity of the soil in the study area is low with regard to the proportions of clay, silt and sand respectively 13%, 7% et 80%.

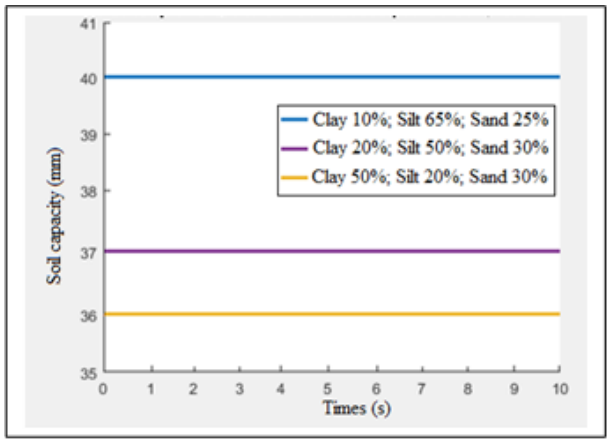


Fig. 14: Temporal Profiles Soil Capacity Depending on the Proportion of Clay, Silt and Sand.

4.2. Characteristics of the photovoltaic field

Figures 15 and 16 respectively represent the curves of the current-voltage I(V) and power-voltage characteristic P(V) of the PV field. These curves are obtained from the simulation of the Simulink model of the photovoltaic field designed in the previous paragraphs. The profiles of the curves conform to those in the literature. We note that under standard operating conditions, the current corresponding to the maximum power point is 34 A and the voltage is 48 V. This voltage corresponds to the boost input voltage.

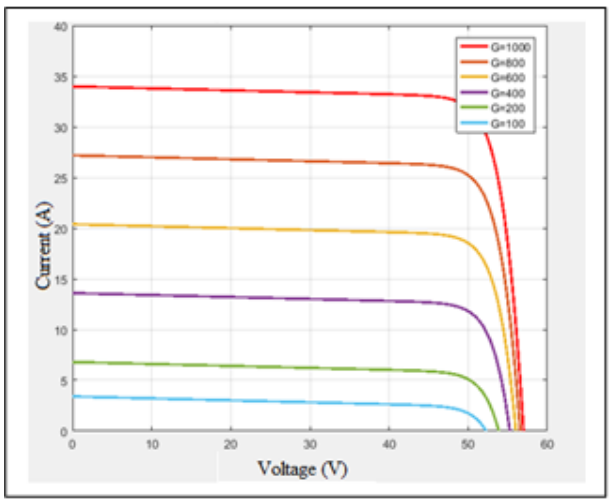


Fig. 15: Current-Voltage Characteristic of the PV Field.

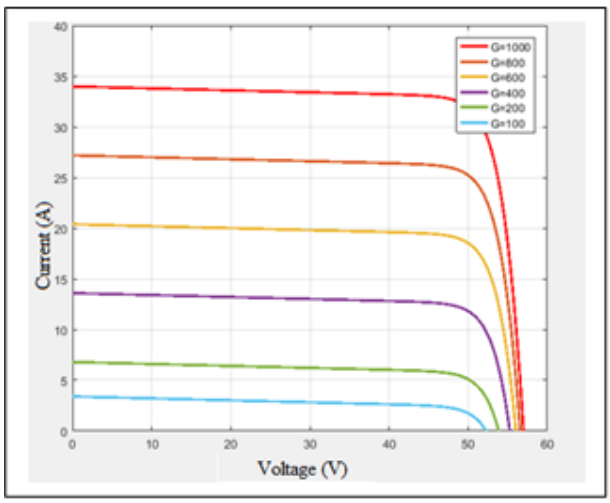


Fig. 16: Power-Voltage Characteristics of the PV Field at Temperature=25°C and Variable Irradiance.

4.3. Pump parameters

Figures 17, 18 and 19 respectively represent the time profiles of the voltage, the current and the rotation speed, which are the operating parameters of the centrifugal pump. The simulation of the system allows us to observe that the Boost converter delivers a voltage of 110 V to the pump which corresponds well to the nominal supply voltage of the pump. At this supply voltage, the rotation speed of the motor

in steady state is 3300 rpm, as can be observed in Figure 17. Figure 18 shows the profile of the current absorbed by the pump. We can observe that the starting current is significant and reaches 55 A which corresponds to approximately four times the nominal current of the motor. In steady state, this current stabilizes at around 13.8 A, approximately equal to the value of the motor's nominal current. These results demonstrate the normal functioning of the system thus modelled.

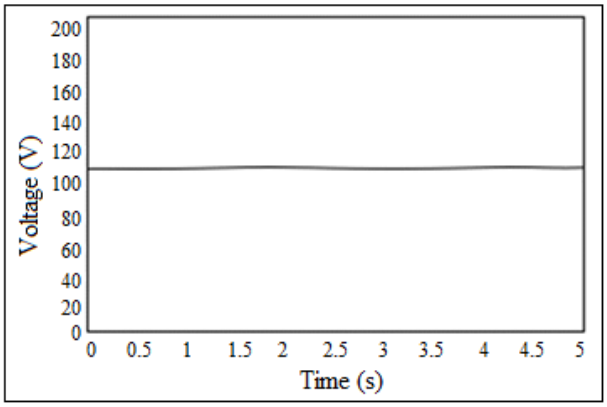


Fig. 17: Voltage Time Profile.

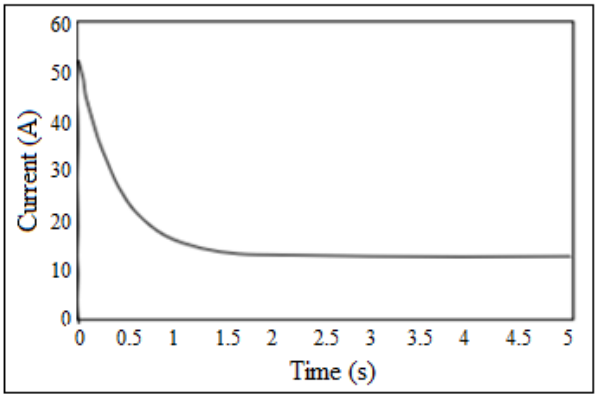


Fig. 18: Current Time Profile.

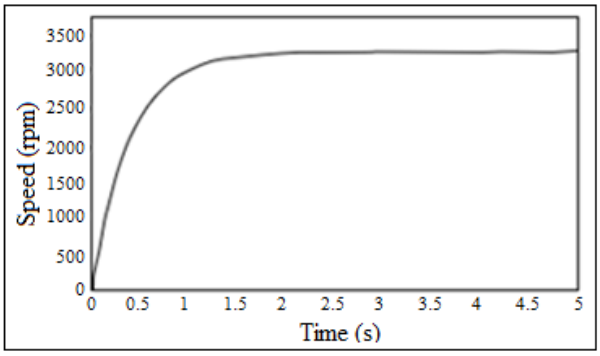


Fig. 19: Rotation Speed Time Profile.

4.4. Variation of dripper function of pump flow

The curves in Figure 20 below represent the flow rate delivered by each dripper (QG) of the irrigation network as a function of the pump flow rate (Q). It can be observed that the flow rate of the dripper increases with the flow rate of the pump. At the maximum flow rate of the centrifugal pump, i.e., 36 m^3/h, the flow rate of the dripper is 20 liters/h. This dripper flow rate is applicable for periods when the water demand of the onions is greater. The configuration of the system thus modeled makes it possible to offer a wide range of flow rates for the taster thanks to the variation in the flow rate of the centrifugal pump.

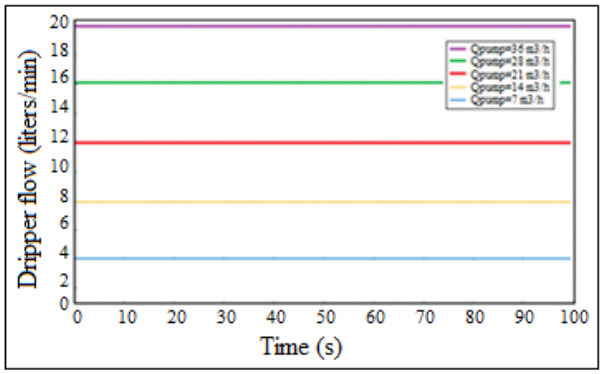


Fig. 20: Dripper Flow Time Profile.

5. Conclusion

The results of this research work are obtained on the basis of preliminary field work such as taking soil samples, determining the proportions of clay, sand and silt, using data collected from farmers in the area study, and simulation results on Matlab/Simulink. The analysis of the soil taken in the study area shows the predominance of sand; the capacity of the soil is therefore low. For a cultivable area of 7200 m, a photovoltaic field of 1600 Watt peak is sufficient to provide the quantity of water useful to the onions for a dripper flow rate of 15 liters/minute. The system thus modeled has the advantage of being autonomous, modular and powered by a clean and renewable energy source. It is therefore beneficial for farmers to have such a system to popularize off-season crops in order to overcome the constraints presented by seasonal crops. Once installed, the system requires very little maintenance and can be used even by non-expert personnel. Which justifies its application even in the most remote areas.

References

[1] ARID (2007). Amélioration des performances des périmètres irrigués en Afrique (APPIA Project). Ouagadougou, Association Régional d'irrigation et Drainage en Afrique de L'ouest et Central (ARID).
[2] Ayangma, F., Nkeng, G.E., Bonoma, D.B. and Nganhou, J. (2008) Evaluation du potentiel en énergie solaire au Cameroun : Cas du Nord Cameroun. African Journal of Science and Technology, 9, 32-40.
[3] Banque mondiale, Rapport 2020 sur la pauvreté et la prospérité partagée., https://www.banquemondiale.org/fr/understanding-poverty.
[4] Bouadi Abed et al., Simulation du Couplage Directe d'un moteur à Courant Continue à un Générateur Photovoltaïque pour le Pompage Agricole, 2015.
[5] Diwediga Badabaté, Hounkpe Koffi, WalaK pérkouma, Batawila Komlan, Tatoni Thierry1 et Akpagana Koffi. Agriculture de contresaison sur les berges de l'oti et ses affluents, African Crop Science Journal, Vol. 20, Issue Supplement s2, pp. 613 – 624, 2012
[6] Elmahni L., Bouhouch L., and Moudden A. Smart management of a photovoltaic pumping station located in the Agadir region. International Journal of Innovation and Applied Studies. ISSN 2028-9324 Vol. 18 No. 4 Dec. 2016, pp. 1216-1227
[7] Maud Du Jardin d'Alekil, Le sol : amendements, engrais, compost, TERRA 2022
[8] Moussi A., Saadi A. Etude comparative entre les techniques d'optimisation des systèmes de pompage photovoltaïque, LARHYSS Journal 1: 157-168. Mai 2001.
[9] M'Biandoun M., Essang T. Importance économique de l'oignon cultivé sur billons sur terrain plat avec irrigation à la raie. TROPICULTURA, 2008, 26, 2, 70-73
[10] Philippe Duchaufour, Pierre Faivre, Jérôme Poulenard, Michel Gury. Introduction à la science du sol, Sol, végétation, environnement 7e édition, Dunod, Paris, 2018
[11] Richard G. ALLEN, Luis S. PEREIRA, Dirk RAES, Martin SMITH. Crop Evapotranspiration (guidelines for computing crop water requirements), FAO Irrigation and Drainage Paper No. 56, 2006.
[12] Sieffermann G., Carte Pédologique du Nord-Cameroun au 1150.000e feuille Pitoa, 1964
[13] Youssouf Dembele, Jean Duchesne, Sibiri Ouattara, Zachari Zida. Evolution du besoin en eau du riz irrigué en fonction des dates de repiquage. Cahiers agriulteurs, 1999, 8 ;93-9.